

[Chem. Pharm. Bull.]  
[29(9)2675-2682(1981)]

## Difference in Physico-Pharmaceutical Properties between Crystalline and Noncrystalline 9,3''-Diacetylmidecamycin<sup>1)</sup>

TOYOMI SATO,\*<sup>a</sup> AKIRA OKADA,<sup>a</sup> KEIJI SEKIGUCHI,<sup>b</sup> and YASUYUKI TSUDA<sup>b</sup>

*Pharmaceutical Development Laboratories, Meiji Seika Kaisha, Ltd.,<sup>a</sup> 580, Horikawa-cho, Saiwai-ku, Kawasaki, 210, Japan and School of Pharmaceutical Sciences, Kitasato University,<sup>b</sup> 9-1, Shirokane 5-chome, Minato-ku, Tokyo, 108, Japan*

(Received January 30, 1981)

The noncrystalline solid form of 9,3''-diacetylmidecamycin (MOM), a new macrolide antibiotic obtained by chemical modification of midecamycin, was prepared by spray-drying and the difference in physico-chemical properties between the crystalline and noncrystalline forms was investigated.

In differential scanning calorimetry (DSC) measurements, the noncrystalline solid always showed two DSC peaks in the curves; one exothermic and the other endothermic. These are attributable to crystallization and melting, respectively.

The apparent solubility of the noncrystalline solid could be determined in 0.2% hydroxypropylmethylcellulose solution but not in water and was much greater than that of the crystalline solid. When the residue during solubility measurements in water was monitored periodically by X-ray diffractometry, the noncrystalline solid was found to convert gradually to the less soluble crystalline form; that is, the former was metastable in aqueous suspension. The conversion rate was distinctly temperature-dependent and the higher the temperature, the faster the crystallization occurred. Also, it was confirmed that the solubility of both the crystalline and the noncrystalline solid increased as the temperature was decreased. From the slopes of the van't Hoff plots, the heat of solution was estimated to be  $-10.9$  kcal/mol for the crystalline solid and  $-7.3$  kcal/mol for the noncrystalline solid.

In addition, the appearance and the surface area of the noncrystalline solid obtained by spray-drying were examined by electron microscopy and by BET gas adsorption analysis. The spray-drying procedure increased the specific surface area to about four times that of the original crystals.

It is considered that the noncrystalline MOM should have a better bioavailability than the crystalline form *in vivo*.

**Keywords**—antibiotic; midecamycin derivative; 9,3''-diacetylmidecamycin; noncrystalline solid; solubility; crystallization; thermal behavior

9,3''-Diacetylmidecamycin<sup>2)</sup> (MOM) is a new 16-membered macrolide antibiotic derivative, in which the hydroxyl groups of midecamycin are acetylated at the C<sub>9</sub> position of the lactone ring and the C<sub>3</sub>'' of mycarose.<sup>3)</sup> MOM has a molecular formula of C<sub>45</sub>H<sub>71</sub>NO<sub>17</sub>, a molecular weight of 897.07, and a melting point of *ca.* 220°C. It is very soluble in methanol, acetone, and chloroform, and very slightly soluble in water. MOM is well tolerated organoleptically when given orally because it has no bitter taste. Its chemical structure is shown in Fig. 1.

Recently, the dissolution behavior of drugs in solid form has attracted the interest of investigators because of its influence on the biological availability of drugs, from the physico-chemical and biopharmaceutical viewpoints. The solubility properties of a solid dosage form of a drug are influenced by its physical state, including polymorphism, hydrate or solvate formation, and degree of crystallinity.

It has been reported that solid drug products having the same chemical composition differ in their physico-chemical properties as a function of their crystalline modifications, resulting in differences in their bioavailability.<sup>4)</sup> Nelson suggested, after oral administration of a solid drug to dogs, that the dissolution rate often regulates the absorption of the drug.<sup>5)</sup> The relationship between the dissolution behavior of the different solid states of a drug and



1) **Crystalline Solid:** The crystalline solid was synthesized according to the method reported by Inouye,<sup>2)</sup> and recrystallized from isopropyl alcohol. The crystalline solid thus obtained was dried at 50–60°C under reduced pressure.

2) **Noncrystalline Solid:** The noncrystalline solid was obtained by the spray-drying of trichloroethane solution of MOM (Freund Co., Ltd.; type FS-50; spray, nozzle type; drying temp., *ca.* 130°C). In this process, ethyl cellulose (EC) was added at 9.1% to give a stable noncrystalline solid. The general properties of both forms are shown in Table I.

**X-Ray Powder Diffractometry**—The instrument used was a Rigaku Geigerflex 2027 X-ray powder diffraction analyzer (Cu-K $\alpha$  radiation,  $\lambda = 1.542 \text{ \AA}$ ; Ni filter).

**Infrared Spectroscopy (IR)**—A Hitachi model 260-10 infrared spectrophotometer was used.

**Scanning Electron Microscopy**—A Jasco JSM 15 scanning electron microscope was used.

**Measurement of Specific Surface Area**—A BET gas adsorption apparatus (model P-600, Shibata Chemical Apparatus Mfg. Co., Ltd.) was used.

**Differential Scanning Calorimetry (DSC)**—DSC measurements were done under semi-closed conditions using a Perkin-Elmer DSC-1B differential scanning calorimeter.

**Solubility Measurement**—The solvent (either distilled water or 0.2% hydroxypropylmethylcellulose (HPMC) aqueous solution (200 ml)) was placed in a water-jacketed cell, and stirred at 700 rpm. After the temperature of the solvent medium had stabilized at the required value, 1 g of sample powder was added to the cell. At appropriate time intervals, solution samples were removed using a volumetric pipet kept at the medium temperature. The sample solution was immediately filtered through a 0.22  $\mu\text{m}$  membrane filter (Millipore Corporation). The concentrations of the sample solutions were determined using an ultra-violet spectrophotometer (Carl Zeiss, type PMQ3) at a wavelength of 231 nm.

**Determination of Biological Activity**—The conventional cup method was applied using *Micrococcus luteus* ATCC 9341 as a test strain.

**Thin-Layer Chromatography (TLC)**—TLC on a silica gel plate (Keiselgel 60, Merck Co., Ltd.) was carried out by using a mixture of benzene-acetone (2:1) as a developing solvent. A 50  $\mu\text{l}$  aliquot of methanol solution of each sample material was spotted on the plate and after development, spots were detected by spraying 10%  $\text{H}_2\text{SO}_4$  solution.

## Results and Discussion

The noncrystalline solid was identified by X-ray powder diffractometry and polarizing microscopy. No definite diffraction peaks were apparent in the X-ray pattern of the noncrystalline solid, and it also showed no polarization. As can be seen in Table I, the biological activity of this solid is not decreased by the process of spray-drying. Further, the TLC behavior of the noncrystalline solid was identical to that of the crystalline solid.

### X-Ray Powder Diffractometry and IR Spectra

Fig. 2 shows the X-ray diffraction patterns of the crystalline and noncrystalline solids. There are distinct differences between them, which can be attributed to the difference in molecular arrangement between the two solids.

As is shown in Fig. 3, the IR spectra of the crystalline and noncrystalline solids were practically indistinguishable, though the spectrum of the crystalline solid showed some evidence of increased intensity at several points.

### Scanning Electron Microscopy and Specific Surface Area

A qualitative assessment of the powder surface of the crystalline and noncrystalline solids was made by means of scanning electron microscopy, as shown in Fig. 4. The photomicrographs indicate distinct differences in the surface characteristics of each powder; that is, the crystalline solid has a hexagonal form, whereas the noncrystalline solid is spheroidal. Moreover, as shown in Table II, the specific surface area of the noncrystalline solid was about 4 times larger than that of the crystalline solid.

### Thermal Behavior by DSC

The DSC curves of the crystalline and noncrystalline solids and their 10:1 (MOM:EC) mixture are shown in Fig. 5. The pure noncrystalline solid exhibited an exothermic peak at about 168°C on the DSC curve (c). The sample removed from the DSC furnace immediately

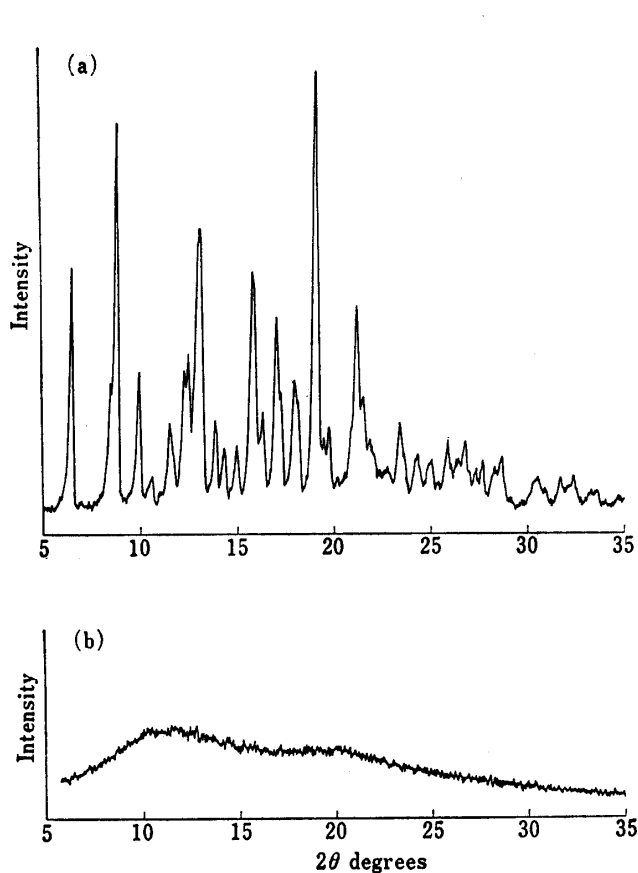


Fig. 2. X-Ray Diffraction Patterns of Crystalline and Noncrystalline Solid Forms of MOM

(a): Crystalline solid.  
(b): Noncrystalline solid.

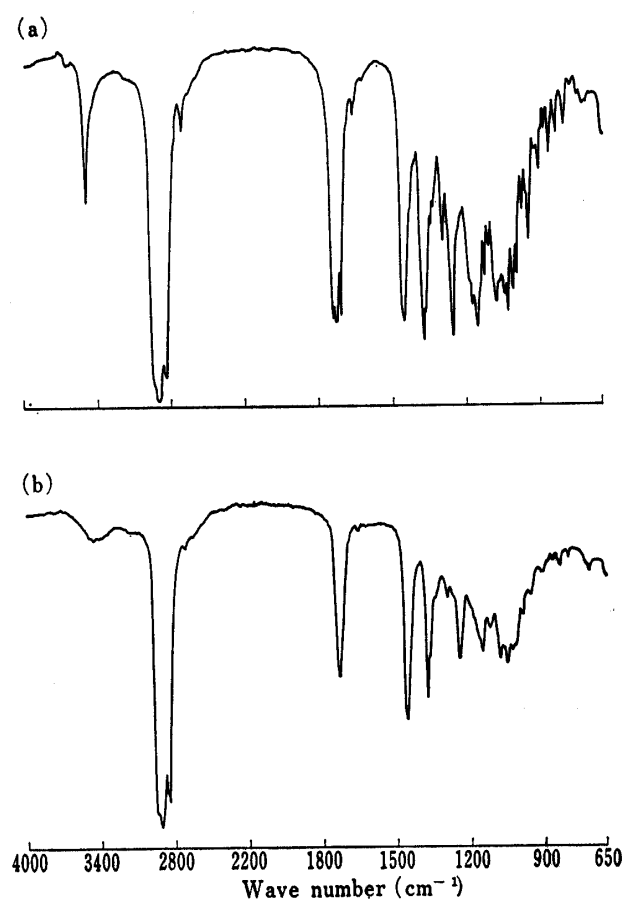


Fig. 3. Infrared Spectra of Crystalline and Noncrystalline Solid Forms of MOM (nujol mull)

(a): Crystalline solid.  
(b): Noncrystalline solid.

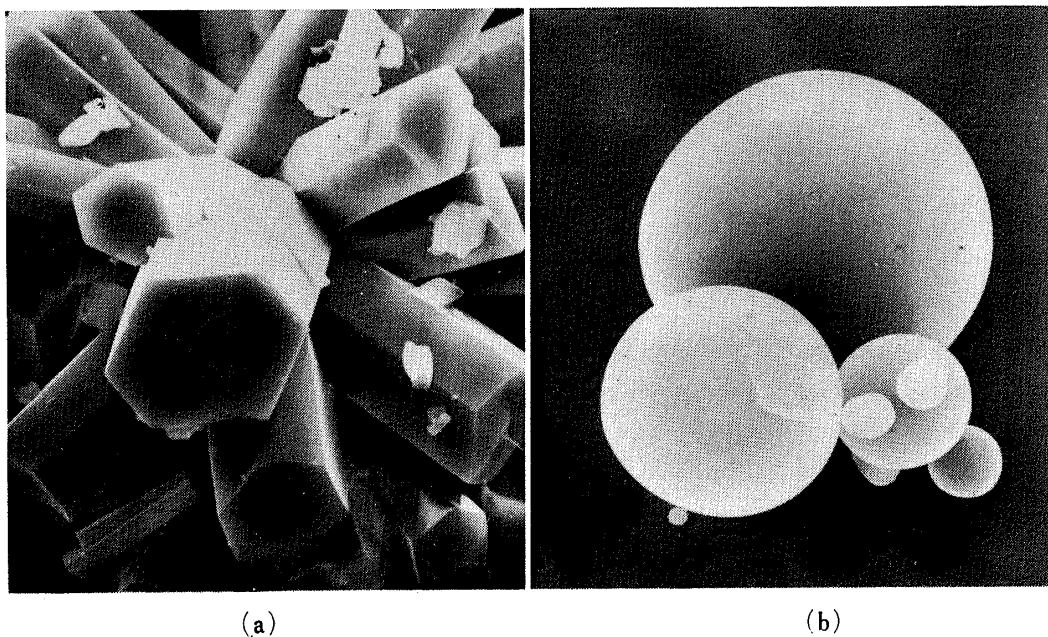


Fig. 4. Electron Micrographs of the Surfaces of Crystalline and Noncrystalline Solids

(a): Crystalline solid.  
(b): Noncrystalline solid with EC.  
Magnification: (a) 1000×, (b) 1000×.

TABLE II. Specific Surface Areas of Crystalline and Noncrystalline Solid Forms of MOM as determined by the BET Method

	Crystalline solid	Noncrystalline solid
Specific surface } areas ( $\text{m}^2/\text{g}$ ) }	0.7	2.7

Sample weight: crystalline solid, 7.17 g; noncrystalline solid, 0.73 g.

after the exothermic peak showed an X-ray diffraction pattern identical to that of the crystalline solid (Fig. 2). Therefore, the first exothermic peak can be attributed to a transition from noncrystalline to crystalline form, while the second peak at about  $227^\circ\text{C}$  is attributable to melting. The crystalline solid, on the other hand, showed only one endothermic peak at about  $227^\circ\text{C}$ , a temperature which is in good agreement with the result obtained by the official method of melting point measurement.<sup>14)</sup> The heats of fusion of both the original crystalline MOM and the heat-transited product of the noncrystalline MOM and the heat of transition were determined to be  $15.3 \pm 0.5$  kcal/mol,  $14.0 \pm 0.7$  kcal/mol, and  $-13.9 \pm 0.6$  kcal/mol, respectively, by measuring the peak areas in at least seven DSC curves of each physical form. From these values, it is clear that for the noncrystalline solid the heat of transition is similar to the heat of fusion.

In the case of the 10:1 mixture, the melting peak became broader than that of either pure MOM solid alone, while the peak temperature was the same as in the case of pure MOM solid. Meanwhile, the transition peak in curve (d) shifted about  $10^\circ\text{C}$  higher, but became smaller than that of the pure noncrystalline solid in curve (c). Both the heat of fusion and the heat of transition for the 10:1 (noncrystalline MOM: EC) mixture were calculated to be  $8.7 \pm 0.4$  kcal/mol. This value is about 40% smaller than that of the noncrystalline solid in the absence of EC. These results suggest that EC might play a role in delaying the transition from noncrystalline to crystalline solid.

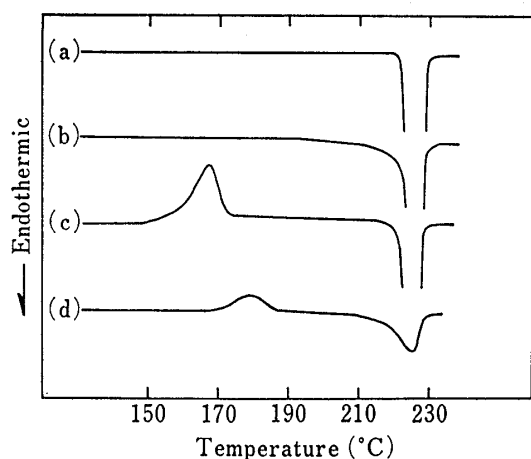


Fig. 5. DSC Curves of Crystalline and Noncrystalline Solids and Their 10:1 (MOM: EC) Mixture under Semi-closed Conditions

- (a): Pure crystalline solid; sample weight, 5.94 mg; heating rate,  $8^\circ/\text{min}$ .
- (b): The 10:1 crystalline solid-EC mixture; sample weight, 5.53 mg; heating rate,  $8^\circ/\text{min}$ .
- (c): Pure noncrystalline solid; sample weight, 6.22 mg; heating rate,  $8^\circ/\text{min}$ .
- (d): The 10:1 noncrystalline solid-EC mixture; sample weight, 2.03 mg; heating rate,  $8^\circ/\text{min}$ .

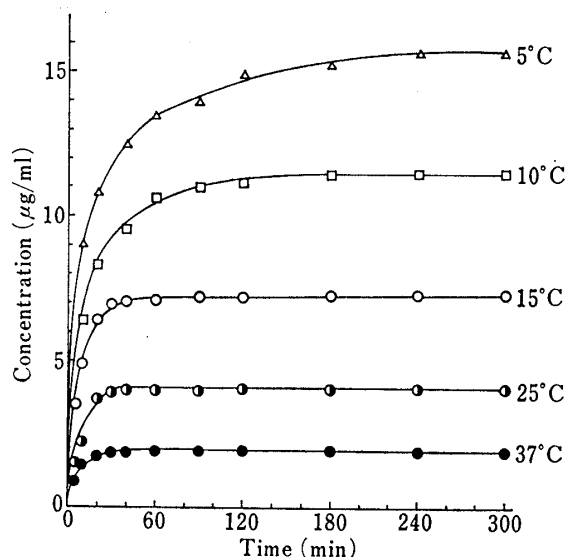


Fig. 6. Concentration-Time Curves for Crystalline Solid MOM in Distilled Water at Various Temperatures

## Solubility

It is well known that a noncrystalline solid, in general, possesses a higher energy level. Therefore, a higher solubility will be obtained than with a crystalline solid of the same substance. However, it is difficult to measure accurately the solubility of the noncrystalline solid because of the conversion to the crystalline form during the solubility experiment. For this reason, few reports have been published on the solubility of noncrystalline solids. In the present investigation, accordingly, the physical state of the noncrystalline solid in solution was examined by X-ray powder diffractometry, whenever its solubility was measured.

Dissolution curves for the crystalline and noncrystalline MOM are shown in Figs. 6, 7, and 8. As to the relationship of solubility and temperature, the solubility of crystalline and noncrystalline MOM increased as the temperature was decreased. The equilibrium solubilities of the crystalline solid in distilled water were 16.0  $\mu\text{g}/\text{ml}$  at 5°C, 11.8  $\mu\text{g}/\text{ml}$  at 10°C, 7.5  $\mu\text{g}/\text{ml}$  at 15°C, 4.3  $\mu\text{g}/\text{ml}$  at 25°C, and 2.1  $\mu\text{g}/\text{ml}$  at 37°C, as shown in Fig. 6. These values were in good accord with the solubility in 0.2% HPMC aqueous solution. Therefore, HPMC has practically no influence on the solubility of MOM.

In the case of the noncrystalline solid, its dissolution curves in distilled water declined gradually after 120, 30, and 20 minutes at 15, 25, and 37°C, respectively, as shown in Fig. 7. In 0.2% HPMC aqueous solution, however, no decrease in solubility occurred with the passage of time, and its solubility was 176.5  $\mu\text{g}/\text{ml}$  at 5°C, 129.7  $\mu\text{g}/\text{ml}$  at 10°C, 99.9  $\mu\text{g}/\text{ml}$  at 15°C, 65.6  $\mu\text{g}/\text{ml}$  at 25°C, and 44.7  $\mu\text{g}/\text{ml}$  at 37°C, as shown in Fig. 8. These figures indicate that the noncrystalline solid had much higher solubility than the crystalline solid at each temperature. The decrease in solubility of the noncrystalline solid in distilled water corresponded well to the appearance of the X-ray diffraction peak, as seen in Fig. 9(a). It was also confirmed that the crystallization rate varied considerably, depending on the temperature; the lower the temperature, the slower the crystallization of the noncrystalline solid in distilled water.

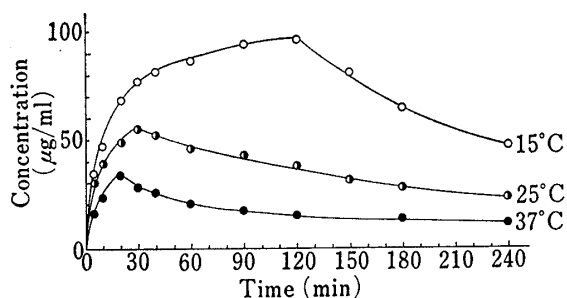


Fig. 7. Concentration-Time Curves for Non-crystalline Solid MOM in Distilled Water at Various Temperatures

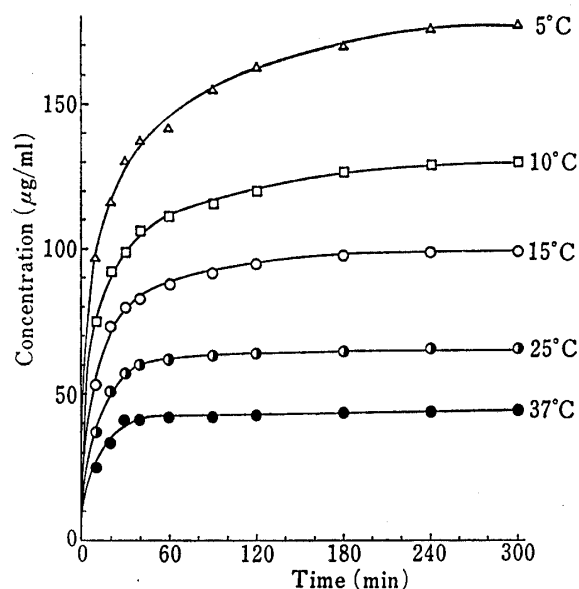


Fig. 8. Concentration-Time Curves for Non-crystalline Solid MOM in 0.2% HPMC Aqueous Solution at Various Temperatures

Meanwhile, there were no changes in X-ray pattern of the solid in the 0.2% HPMC aqueous solution, as shown in Fig. 9(b). It was concluded that partial crystallization of the noncrystalline solid occurred in distilled water, whereas in the 0.2% HPMC solution, the crystallization was suppressed completely, presumably due to the higher viscosity. Accordingly, the dissolution curve in the 0.2% HPMC aqueous solution at each temperature was verified to be the

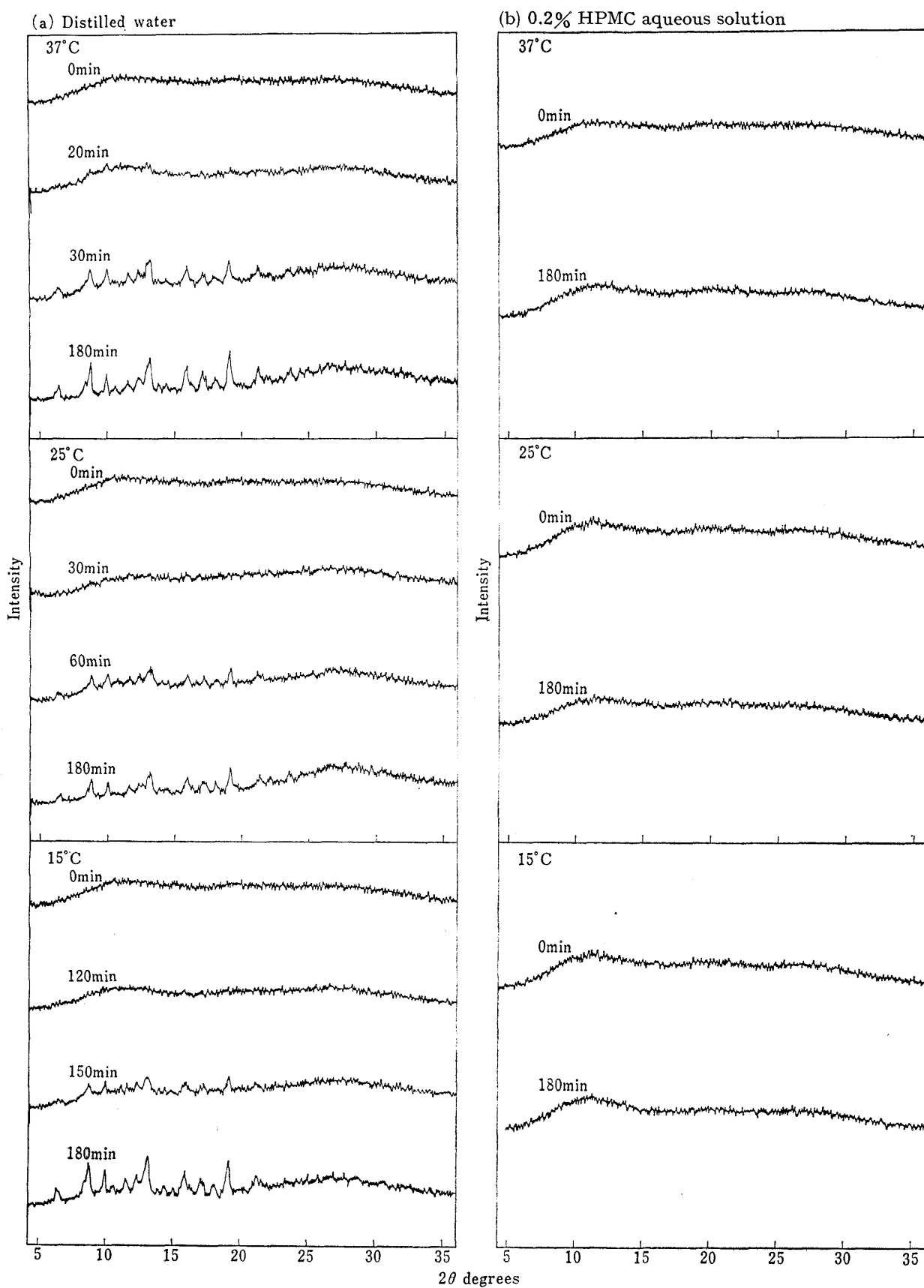


Fig. 9. Phase Conversion of Noncrystalline Solid MOM in Distilled Water and 0.2% HPMC Aqueous Solution during Solubility Measurements at Various Temperatures

equilibrium solubility. Figure 10 shows the van't Hoff plots for these data with the curves determined by the least-squares method. The fitted curves indicate heats of solution of  $-10.9$  kcal/mol for the crystalline solid and  $-7.3$  kcal/mol for the noncrystalline solid.

### Conclusions

1. A stable noncrystalline solid form of MOM was successfully prepared by spray-drying of its trichloroethane solution in the presence of EC.

2. The absence of any chemical reaction between MOM and EC was confirmed by bioassay, TLC, and DSC. In other words, exactly the same bioactivity was demonstrated for both MOM and the MOM-EC mixture.

3. The noncrystalline solid containing EC did not convert to a crystalline solid during solubility measurements in 0.2% HPMC solution; it showed an intrinsic solubility.

4. The noncrystalline solid was at least ten times more soluble in 0.2% HPMC solution than was the crystalline solid. This difference in solubility can be utilized to increase the bioavailability of MOM *in vivo*.

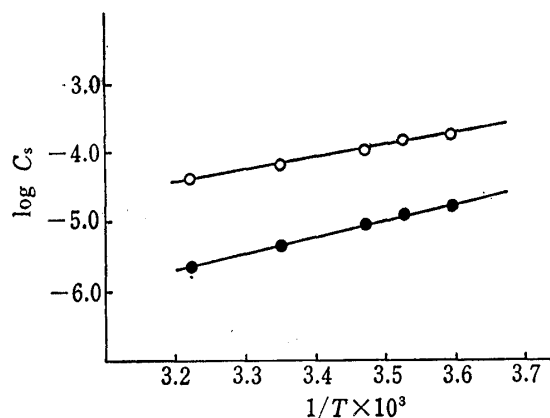


Fig. 10. The van't Hoff Plots of Solubility Values for Crystalline and Noncrystalline Solid Forms of MOM in 0.2% HPMC Aqueous Solution

○—○: noncrystalline solid.  
●—●: crystalline solid.

### References and Notes

- 1) This paper forms Part I of "Physico-Pharmaceutical Studies on 9,3"-Diacetylmidecamycin."
- 2) S. Omoto, K. Iwamatsu, S. Inouye, and T. Niida, *J. Antibiot. (Tokyo)*, **29**, 536 (1976).
- 3) T. Niida, T. Tsuruoka, N. Ezaki, T. Shomura, E. Akita, and S. Inouye, *J. Antibiot. (Tokyo)*, **24**, 319 (1971).
- 4) A.J. Aguiar, J. Krc. Jr., A.W. Kinkel, and J.C. Samyn, *J. Pharm. Sci.*, **56**, 847 (1967); A.J. Aguiar, and J.E. Zelmer, *J. Pharm. Sci.*, **58**, 983 (1969); J.W. Poole, G. Owen, J. Silrerio, J.N. Freyhof, and S.B. Rosenman, *Current Therap. Res.*, **10**, 292 (1968); J. Halebian, and W. McCrone, *J. Pharm. Sci.*, **58**, 911 (1969).
- 5) B.E. Ballard and E. Nelson, *J. Pharmacol. Exper. Therap.*, **135**, 120 (1962).
- 6) G. Levy, *J. Pharm. Sci.*, **50**, 388 (1961); W. Morozowich, T. Chulski, W.E. Hamlin, P.M. Jones, J.I. Northam, A. Purmalis, and J.G. Wagner, *J. Pharm. Sci.*, **51**, 993 (1962).
- 7) J.D. Mullins and T.J. Macek, *J. Am. Pharm. Assoc.*, **49**, 245 (1960).
- 8) L. Almirante, I. DeCarneri, and G. Coppi, *Il Farmaco. Ed. Pr.*, **15**, 471 (1960).
- 9) S. Miyazaki, R. Hori, and T. Arita, *Yakugaku Zasshi*, **95**, 629 (1975).
- 10) E. Shefter and T. Higuchi, *J. Pharm. Sci.*, **52**, 781 (1963).
- 11) M.A. Moustafa, A.R. Ebian, S.A. Khalil, and M.M. Motawi, *J. Pharm. Pharmacol.*, **23**, 868 (1971).
- 12) J.K. Halebian, R.T. Koda, and J.A. Biles, *J. Pharm. Sci.*, **60**, 1485 (1971).
- 13) M. Kanke and K. Sekiguchi, *Chem. Pharm. Bull.*, **21**, 878 (1973).
- 14) J.P. X. 744.